\$ SUPER

Contents lists available at ScienceDirect

Environmental Pollution

journal homepage: www.elsevier.com/locate/envpol





Effects of natural particles on photo-reduction of divalent mercury in everglades waters[☆]

Kang Wang, Guangliang Liu, Yong Cai

Department of Chemistry & Biochemistry and Southeast Environmental Research Center, Florida International University, Miami, FL, 33199, USA

ARTICLE INFO

Keywords: Mercury Photo-reduction Natural particles Everglades waters

ABSTRACT

Photo-reduction of divalent mercury (Hg(II)) in waters plays an important role in the air-water exchange of Hg and biogeochemical cycle of Hg in general. As previous studies on photo-reduction of Hg(II) have mainly focused on dissolved Hg species, the effects of natural particles on photo-reduction of Hg(II) remain largely unknown, except the presumed light attenuating effect through light absorption and scattering. Considering the prevalence of particulate Hg due to adsorption of divalent and elemental Hg species on aquatic particles that are often photochemically active, natural particles may play a more direct role in Hg photo-reduction. By using incubation experiments with Everglades waters and additions of isotopically labelled Hg(II), we studied the effects of particles on photo-reduction of Hg(II) in natural waters. The effect of natural particles on Hg(II) photo-reduction was not observed between filtered or unfiltered Everglades waters, probably because of the low particle concentrations (<3 mg/L). When suspended particles isolated from original water was used to amend its concentration to 6.9 times the ambient Everglades waters, photo-reduction of Hg(II) was significantly enhanced. Given that the particles in Everglades waters are often semiconducting in nature, particulate Hg(II) may undergo heterogenous photo-reduction and lead to higher Hg(II) photo-reduction. However, in Everglades waters with both suspended and settling particles, high concentrations (~100 mg/L) of particles did not result in enhanced Hg(II) photo-reduction. In this case, the enhancing effects of particles on Hg(II) photo-reduction were likely offset by inhibiting effects due to the higher irradiation attenuation and lower Hg(II) partition coefficients of the settling particles with larger sizes. This study highlights the direct involvements of particles in photoreaction of Hg species in natural waters and calls for more mechanistic research on heterogenous photo-reduction of Hg species on particles' surfaces.

1. Introduction

Mercury (Hg) is a notorious contaminant threatening human and environmental health. In the environment, Hg cycles between several different forms (i.e., elemental Hg (Hg(0)), divalent Hg (Hg(II)), and methyl Hg (MeHg)) and major environmental compartments (i.e., air, soil, water, sediment), forming a complicated global biogeochemical Hg cycle. Being emitted from natural and anthropogenic sources, atmospheric Hg(0) has a long lifetime of 6–12 months and can be transported over long distances (Saiz-Lopez et al., 2019). The oxidation of Hg(0) to Hg(II) greatly enhances the deposition of Hg to terrestrial and aquatic environments, while reduction of Hg(II) back to Hg(0) in these environmental compartments strongly facilitates Hg emitting to the atmosphere (Ariya et al., 2015). In aquatic environments, Hg(II) and Hg(0)

are converted via different pathways to MeHg, the more toxic Hg species that biomagnifies in the aquatic food web and poses health risks to top predators (Wang et al., 2022).

As an important part of the global Hg biogeochemical cycle, the airwater Hg exchange controls the pool of Hg(II) and Hg(0) available for MeHg production in aquatic environments and the Hg(0) emission to atmosphere for long range transportation. However, currently the largest potential error of global budget on Hg cycling lies in the air-water Hg exchange (UNEP/AMAP, 2013), largely due to the lack of understanding on Hg redox in water (Qureshi et al., 2011). Although photo-reduction is a major pathway for Hg(II) reduction in surface water, our knowledge towards this process is far from satisfactory and mainly limited to reactions of dissolved Hg species (Luo et al., 2020). The ubiquitous presence of particulate Hg(II) and Hg(0) in natural

E-mail address: cai@fiu.edu (Y. Cai).

 $[\]ensuremath{^{\star}}$ This paper has been recommended for acceptance by Sarah Harmon.

^{*} Corresponding author.

waters suggests that natural particles likely play an important role in the Hg(II) photo-reduction process (O'Driscoll et al., 2018; Wang et al., 2015). However, only few studies have investigated the effects of natural particles on photo-reduction of Hg(II) in aquatic environments (Luo et al., 2020; Vost et al., 2012). Generally, particles in natural waters are believed to inhibit photo-reduction of Hg(II) through two mechanisms: 1) changing the quality and intensity of solar irradiation (Costa and Liss, 2000) via absorbing or scattering lights (Castelle et al., 2009; Vost et al., 2012); 2) controlling the dissolved Hg(II) available for photo-reduction in waters through adsorption (Tseng et al., 2004). However, some studies did observe higher photo-reduction of Hg(II) in waters with natural particles than in filtered waters (Amyot et al., 1997; Rolfhus and Fitzgerald, 2004). For examples, when studying dissolved gaseous mercury (DGM, mainly composed of Hg(0)) in coastal seawater from the Gulf of Mexico, Amyot et al. (1997) observed over 40% higher production of DGM in unfiltered waters than in filtered waters during a 7-h incubation under daylight. This suggests that natural particles may play other roles and enhance photo-reduction of Hg(II) (Amyot et al., 1997), in addition to its indirect involvements in affecting light penetration and photo-reducible Hg(II).

It has been hypothesized that natural particles may play a more direct role in Hg(II) photo-reduction, which may proceed heterogeneously on particles' surfaces (Nriagu, 1994). As a possible mechanism, photoexcitation of natural sensitizers (e.g., organic matter) in particles from natural waters could produce free radicals and reactive oxygen species (Wu et al., 2022), which may react with particulate Hg species to accomplish Hg(II) reduction (e.g., O₂[•]) (Li et al., 2020) and Hg(0) oxidation (e.g., OH) (Hines and Brezonik, 2004). For the role of particles in Hg(II) reduction, a more plausible mechanism involves semiconducting particles (Nriagu, 1994). In natural waters, particles often contain minerals with semiconducting properties, including some metal oxides and sulfides like TiO2, Fe-oxides, Mn-oxides, Al2O3, ZnO, ZnS and FeS₂ (Litter et al., 1991). Under irradiations with wavelengths short enough, the semiconducting particles are excited to produce pairs of photo-electron and photo-hole possessing the reducing power of the conduction band (CB) edge and the oxidizing power of valence band (VB) edge, respectively (Starr et al., 2017). The redox couples of Hg species ($E_{Hg(II)/Hg(I)}^0 = 0.91 \text{ V}$, $E_{Hg(I)/Hg(0)}^0 = 0.79 \text{ V}$, and $E_{Hg(II)/Hg(0)}^0 = 0.79 \text{ V}$ 0.85 V) are well within the band gaps (E_{bg}) of many aquatic particles (Chen and Wang, 2012), such as pyrite (FeS₂, $E_{bg} = 0.95$ eV), hematite (α -Fe $_2$ O $_3$, E $_{bg}=$ 2.2 eV), ZnO (E $_{bg}=$ 3.2 eV), and anatase (TiO $_2$, E $_{bg}=$ 3.2 eV). Therefore, the strong reducing photo-electrons would reduce Hg (II) while the strong oxidizing photo-holes would oxidize Hg(0). In natural waters, particles are often coated with organic ligands which can effectively scavenge photo-holes, thus inhibiting their oxidizing of Hg(0) and promoting Hg(II) reduction. Previous studies have confirmed the heterogeneous photo-reduction of Hg(II) in artificial media with engineered particles of TiO2 (Hegyi and Horvath, 2004; Skubal and Meshkov, 2002; Wang et al., 2004). The results show that the heterogeneous photo-reduction rates are controlled by a group of parameters, including characteristics of TiO2 particles like concentration, size and surface coating, irradiation properties like intensity and wavelength, pH, and photo-hole scavengers (Zhang, 2006). More recent studies have reported photo-reduction of Hg(II) in aqueous solution with synthesized particles containing α-Fe₂O₃ or ZnO (Kadi et al., 2020; Mohamed and Ismail, 2021). Notably, the Hg(II) photo-reduction was greatly enhanced in solutions with mesoporous heterojunction of $\alpha\text{-Fe}_2O_3/g\text{-}C_3N_4$ and α -Fe₂O₃/ZnO than those with pure nanoparticles of α -Fe₂O₃ and ZnO. However, it remains to be verified whether the Hg(II) photo-reduction involving semiconducting particles occurs in natural waters (Saniewska et al., 2014).

The objective of this study was to investigate the effects of natural particles on photo-reduction of Hg(II) in natural waters, particularly the potential occurrence of heterogeneous Hg(II) photo-reduction on particles' surfaces. To fulfill the purpose, we carried out Hg(II) photo-reduction experiments with Everglades waters and additions of

isotopically labelled Hg(II). Based on the experiments with different settings of waters, we discussed the effects of particles on photoreduction of Hg(II) in Everglades water. While the particles' characteristics (i.e., concentrations, particle size distribution, and particle composition) were consistent in waters with the same setting, these characteristics differed with the different settings of waters used for experiments.

2. Materials and methods

2.1. Experimental preparation

The waters used for photo-reduction experiments were collected from the Everglades National Park. Given the spatial and temporal variations of water chemistry in the Everglades National Park (Jiang et al., 2018; Liu et al., 2008), water samples were collected at Site 1 and 2 on April 20 and August 4, 2021, respectively (Fig. S1). The waters collected from Site 2 were with high concentrations of settling particles, due to the sediments disturbance and re-suspension caused by heavy rain right before sampling. When collecting waters, sampling personnel wore nitrile gloves and followed the "Clean hands-dirty hands" protocol to prevent potential contamination (Fitzgerald, 1999). Water samples were collected into precleaned 2-L Teflon bottles (Hammerschmidt et al., 2011), which were rinsed with the waters to be sampled for three times. The sampled waters were immediately transported to the Cai Lab for Environmental Bioinorganic Chemistry at Florida International University. For pH of the water samples, measurements were conducted on site using an Orion pH electrode (Thermal Fisher). The concentrations of particles were measured with gravitation method as detailed in Section 2.2. Dissolved organic carbon (DOC) and total organic carbon (TOC) concentrations were measured by Pt catalyzed high temperature combustion on a Shimadzu TOC analyzer.

Prior to their usage in Hg(II) photo-reduction experiments, the Everglades waters received treatments of sterilization, filtration, and particle amendments (Fig. 1). Sterilization of the water at 121 °C for 20 min (Steris Amsco Lab 250 Steam Sterilizer) inactivated biological activities that may contribute to Hg(II) reduction (Kritee et al., 2008), although the occurrence of water chemistry changes might be involved in the process. Filtration with 0.45 µm PTFE filters (Millipore, 47 mm) removed particles from the Everglades water. Amendments of particles were performed in different manners to reach higher concentrations (Table S1). For waters from Site 1, the suspended particles were amended to higher concentrations by releasing particles retained on PTFE filters through a 24-h stirring period under dark. The period was within 2 h from starting filtration to putting the loaded filters back into water for particle release. Suspended particles amended to higher concentration by re-suspension exhibited a similar pattern of size distribution as that of suspended particles at original concentration (Fig. S2). The waters from Site 2 were left to stand for 24 h for some particles to settle down. Here we regarded the settled particles as settling particles. Then the supernatant was decanted to represent waters with suspended particles. Both suspended and settling particles were present in the original waters, which represented waters with amendments of particles.

After the treatments, 100 mL of the treated waters was transferred into each pre-cleaned quartz bubbler. The ²⁰²Hg enriched Hg(II) was then added into the bubblers to reach a target concentration of 20 ng/L. The ²⁰²Hg(II) stock solution (²⁰²Hg(NO₃)₂, 100 mg/L) was prepared by dissolving 10 mg of elemental ²⁰²Hg (Oak Ridge National Laboratory, ²⁰²Hg > 98%) in 5 mL of concentrated HNO₃ (trace metal clean grade, Sigma-Aldrich) (Southworth et al., 1958), and diluting with 95 mL Milli-Q water (Element Grade, Millipore) in a pre-cleaned 125 mL Teflon bottle (Cotton and Wilkinson, 1962; Pataki and Zapp, 2013). Water in the bubblers were stirred with a Teflon-coated stir bar for 18 h under dark for the added ²⁰²Hg(II) to reach equilibrium with particles and DOC (Lamborg et al., 2003; Le Roux et al., 2001). Our preliminary

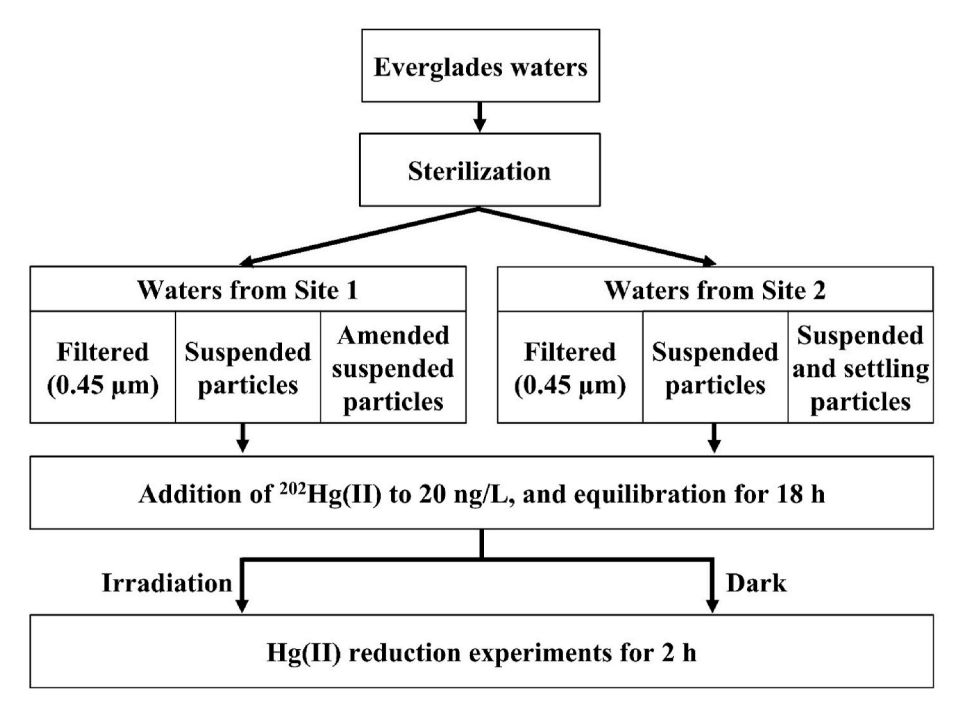


Fig. 1. Flow-chart of procedures for Hg(II) reduction experiments using Everglades waters.

experiments show that Hg(II) in waters stayed at the same concentrations throughout the equilibration process, demonstrating that reduction of Hg(II) did not occur during the equilibration under dark.

2.2. Mercury(II) photo-reduction experiments

The experiments for Hg(II) photo-reduction were carried out in the quartz bubblers with simulated sunlight (Fig. 2). The irradiation was from a xenon lamp in a solar simulator (Suntest XLS+), with the intensity set at 765 W/m 2 that is equivalent to solar radiation in South Florida in November (Moradi et al., 2017). During the 2-h experiments, a Teflon-coated stir bar was used to keep stirring the water in each bubbler, to maintain a homogenous distribution of particles and prevent sinking of settling particles. Meanwhile, N $_2$ was used to purge (40 mL/min) the Hg(0) from Hg(II) reduction in the bubbler to a gold-coated sand trap. Ahead of the bubbler was another gold-coated sand trap to remove the trace Hg from N $_2$ gas cylinder, while a soda lime trap following the bubbler was to dehydrate the outgoing gas. The experiments were started by turning on the solar simulator and beginning

purging with N_2 and terminated by shutting down the solar simulator and N_2 purging. The continuous purging of N_2 was to remove all dissolved Hg(0) from the solutions for recovery by gold-coated sand trap, and to prevent the Hg(0) reduced from Hg(II) from being re-oxidized to Hg(II) (O'Driscoll et al., 2006; Zhang and Lindberg, 2001). After the light was turned off, we switched the existing gold-coated sand trap to a new one and kept purging the system for 20 min. Measurements showed that no Hg(0) was captured by the new traps, confirming that all dissolved Hg(0) was purged to the original gold-coated sand traps. The control experiments were conducted under the same conditions except that the irradiation was absent. During the experiments, temperature of the waters in bubblers was maintained at 21.0 \pm 0.8 °C. Each experiment with the same setting was performed in triplicates.

Given the crucial importance of irradiation in controlling photoreduction of Hg(II), their characteristics were monitored at the bottom of each bubbler. Monitoring of irradiation intensity was carried out with LI-192 Quantum Sensor (LI-COR Biosciences). Because irradiation attenuates differently at different wavelengths when passing through waters in bubblers (Dombrovsky et al., 2011), we monitored the

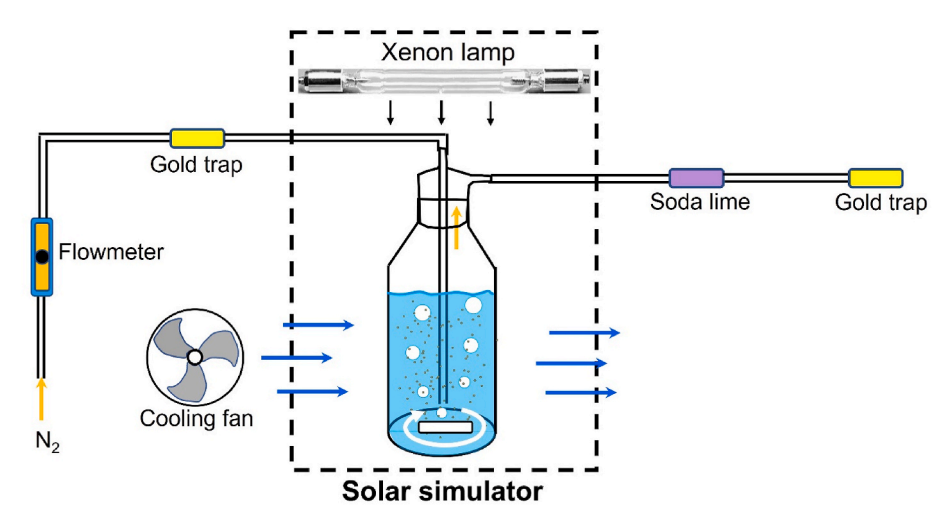


Fig. 2. Setup of experiments for Hg(II) photo-reduction in waters from Everglades.

fractions of ultraviolet (UV), visible light (Vis), and near infrared (NIR). Using a fiber optic spectrometer (AvaSpec-Mini2048CL, Avantes), we measured the irradiation spectrum from 144 nm to 1100 nm. The fractions of UV, Vis, and NIR were calculated by: 1) integrating the irradiation over their corresponding wavelength ranges, and 2) dividing the value to that integrated over the full wavelength span (144–1100 nm). Due to the wavelength limits of spectrum measurements, the UV and NIR were integrated over a narrower wavelength span of 144–400 nm and 780–1100 nm, as opposed to 100–400 nm (Braude, 1955) and 780–2500 nm (Korsman et al., 2002), respectively.

To investigate the effects of particles on Hg(II) photo-reduction, the properties of particles were measured, including concentrations, particle-size distribution and particles' composition (i.e., elemental composition, mineralogy, and metal contents). The particle concentrations were determined by gravitation method. Water samples were filtered with pre-dried (at 60 °C) and weighed PTFE filters. The filters with particles were then dried at 60 °C and weighed (Pućko et al., 2014). The weight difference represented particles' weight, which was then divided by water sample volume to obtain the particles' concentration. Water samples were sent to Particle Technology Labs (PTL, Illinois, USA) for particle-sized distribution measurements. Using the light obscuration and single particle optical sizing technique, technicians at PTL measured the sizes and numbers of particles in waters from 0.5 μm to 422 μm . For the particles' composition, we have measured the elemental composition, mineralogy, and metal contents with different methodologies. The particles' elemental composition was measured with scanning electron microscope with energy-dispersive X-ray spectroscopy (SEM-EDS) at Florida Center for Analytical Electron Microscopy. The particles' mineralogy was measured with X-ray diffraction (XRD) at Mineralogy and Soil Chemistry Laboratory, University of Florida. The particles' metal contents analysis was conducted at the Cai Lab for Environmental Bioinorganic Chemistry at Florida International University. The particles from Everglades water were firstly digested using HNO3, H2O2, and HF, and the digestates were then analyzed with inductively coupled plasma mass spectrometry (ICPMS) for various metals, following standard laboratory procedures modified after EPA method 6020 and method 3050.

We also measured partitioning of Hg species in Everglades waters with different conditions of particles and Hg(II) additions. For Site 1 waters, the settings include: 1) suspended particles and no Hg(II) additions; 2) suspended particles and 20 ng/L of Hg(II) addition; and 3) suspended particles amended to 11.22 mg/L and 20 ng/L of Hg(II) addition. For Site 2 waters, the settings include: 1) suspended particles and no Hg(II) addition; 2) suspended & settling particles and no Hg(II) addition; 3) suspended & settling particles and 4 ng/L of Hg(II) addition; and 4) suspended & settling particles and 20 ng/L of Hg(II) addition. After stirring the treated waters in the bubblers for 18 h under dark, total dissolved Hg and total particulate Hg were separated by filtering the waters with 0.45 µm PTFE filters. While the total dissolved Hg samples were acidified with 1% (v:v) HCl and oxidized with 0.5% (v:v) BrCl, the total particulate Hg samples were digested with 4 N HNO3 for 4 h at 60 °C with intermittent sonication followed by oxidation with BrCl (Munson et al., 2015). Both Hg species were determined with CVAFS method on a PSA mercury analyzer.

2.3. Sample analysis for mercury

Immediately after termination of the experiments, different types of samples were collected for Hg analysis. As Hg(0) adsorbed on particles is non-purgeable, the purgeable Hg(0) collected on the receiving gold-coated sand trap represents DGM, or dissolved Hg(0) (Wang et al., 2015). After filtering the water in bubblers through 0.45 μ m PTFE filters, the filtrate was acidified with 1% (v:v) HCl and oxidized with 0.5% (v:v) BrCl for dissolved Hg(II). The filters retained particles with both particulate Hg(0) and particulate Hg(II), which were discerned following a thermal desorption method based on the fact that the two Hg species are

released at different temperatures from the solid matrix (Liu et al., 2006). By heating the filters with particles to 150 °C and 250 °C, particulate Hg(0) and Hg(II) were released and collected on a gold-coated sand trap, respectively (Wang et al., 2015). It should be noted that thermal desorption is not a precise method in Hg speciation analysis, because particulate Hg(0) or Hg(II) is released within a temperature range that is dependent upon the exact Hg species (e.g., HgCl₂, HgS) and the solid matrix. For example, the particulate Hg(II) may not be totally recovered as part of Hg(II) bound to organic matter might be released at temperatures above 250 °C (Liu et al., 2006).

The Hg species of dissolved Hg(0), particulate Hg(0), and particulate Hg(II) were all in the form of Hg(0) and trapped on gold-coated sand traps. To quantify the Hg isotopes abundances, the traps were heated to 500 °C to release Hg(0) for determination with ICPMS. During this process, Ar was used as carrier gas at the flow rate of 350 ± 50 mL/min. Excessive BrCl in the solutions was destroyed by adding 0.2% (v:v) of NH2OH-HCl, before the analysis of dissolved Hg(II) following the methods involving SnCl2 reduction, purge and trap, and determination with PSA mercury analyzer. To measure Hg isotopes, the Hg(0) exhaust from PSA mercury analyzer was retrieved in gold traps, which were then thermal desorbed and analyzed on ICPMS. The detailed information of the Hg analysis was provided in an earlier study by our research group (Wang et al., 2015).

2.4. Calculation for mercury(II) reduction

The measured Hg isotopes of different Hg species originated from two sources of Hg with different isotopic ratios. One was the Hg isotopes from the added isotopically enriched ²⁰²Hg(II), and the other was those from ambient environments, including Hg in Everglades water and background Hg that may present. For example, the measured dissolved $^{202}\mathrm{Hg}(0)$ was from the $^{202}\mathrm{Hg}(0)$ reduced from the added $^{202}\mathrm{Hg}(\mathrm{II})$, and the ²⁰²Hg(0) from ambient environment which was either originally present as ²⁰²Hg(0) or reduced from ambient ²⁰²Hg(II). For added ²⁰²Hg (II), the isotopic ratios were certified by manufacturer (Oak Ridge National Laboratory). The values from International Union of Pure and Applied Chemistry (Meija et al., 2010) were used as the isotopic ratios for Hg from ambient environments (Tsui et al., 2020). Using a linear matrix inverse approach, we quantified the contributions of different Hg sources in the measured Hg isotopes for all Hg species (Hintelmann and Evans, 1997; Hintelmann and Ogrinc, 2003). In the quantification, ²⁰⁰Hg and ²⁰²Hg were used as the tracer isotopes of the ambient and added Hg, respectively (Wang et al., 2020). Then, reduction of the added ²⁰²Hg(II) was used to calculate the Hg(II) reduction ratios during the Hg (II) photo-reduction experiments. Specifically, Hg(II) reduction ratios were quantified by dividing the formed Hg(0) by the Hg reduction substrate. Here the formed Hg(0) included dissolved and particulate 202 Hg(0) from added 202 Hg(II), while the Hg reduction substrate was the sum of measured 202 Hg(0) and 202 Hg(II) in both dissolved and particulate phases that originated from added ²⁰²Hg(II). In addition to the total reduction ratios as calculated above, we also quantified the separate reduction ratios of dissolved and particulate Hg(0) in the Hg reduction substrate. Here we did not use the theoretical value of added Hg(II) as reduction substrate because of the large range (40.0 \pm 5.4%–97.6% \pm 16.4%) of recoveries for the added ²⁰²Hg(II) (Fig. S3). In experimental waters, the Hg loss can be substantial and not necessarily recovered as Hg(0) (Beucher et al., 2002; Wang et al., 2015). Meanwhile, the possibly underestimated particulate Hg(II) can partly explain the Hg that was not recovered. Despite the potential occurrence of isotope fractionation during the Hg loss, its effects in Hg isotope distribution were in the magnitude of 1% and not considered for calculation of Hg(II) reduction (Tsui et al., 2020).

3. Results and discussion

3.1. Mercury(II) reduction in experiments

Fig. 3 shows the reduction percentages of Hg(II) in Everglades waters from experiments with different settings. In experiments under dark, Hg (II) reduction percentages were 3.6 \pm 1.9% (1.5–5.1%) and 3.2 \pm 2.3% (1.5–5.9%) for waters from Site 1 and 2, respectively. In experiments under irradiation, the Hg(II) reduction percentages were significantly higher (t-test: Site 1, p = 0.029; Site 2, p < 0.001) than under dark, reaching 34.2 \pm 15.6% (23.8–52.1%) and 21.1 \pm 2.1% (18.8–22.9%) for waters from Site 1 and 2, respectively. In the absence of biological activities, photo-reduction was the predominant pathway for Hg(II) reduction in natural waters, whereas the occurrence of reduction under dark was in much lower extents. This agrees well with the prevailing understanding that underlines the major role of Hg(II) photo-reduction, especially when biological activities are absent (Luo et al., 2020). Reduction of Hg(II) under dark has been reported to occur at substantial extents, but such reactions were mediated by microorganisms (Kritee et al., 2008; Lamborg et al., 2021). In our experiments, the low abiotic reduction of Hg(II) under dark likely resulted from the Hg(II) reduction by natural organic matter (Si et al., 2022). Meanwhile, the suspended particles may also be involved in the reactions, as suggested by the higher dark reduction in waters with unamended suspended particles than in filtered water (t-test: Site 1, p = 0.037; Site 2, p = 0.009). Similarly, an earlier study observed production of DGM under dark in unfiltered waters and negligible production in filtered waters (Beucher et al., 2002). The higher DGM production was attributed to occurrence of heterogeneous Hg(II) reduction and particles' involvement in the reactions. Given that the waters were not sterilized, microorganisms may have played a role in the reactions. In our experiments, Hg(II) reduction under dark was also higher in waters with amended particles than in filtered waters, but lacking statistical significance (t-test: Site 1, p=0.060; Site 2, p=0.128). Therefore, the particles might be playing a more complicated role in the abiotic dark reduction that warrants further investigation in the future.

In experiments with irradiation, the Hg(II) reduction occurred at similar extents (t-test, p = 0.62) in filtered waters (26.5 \pm 1.1%) and waters with unamended particles (23.8 \pm 8.6%) from Site 1 (Fig. 3, B). The similar levels of Hg(II) reduction (t-test, p = 0.82) under irradiation was also observed in Site 2 waters without (21.6 \pm 4.4%) and with suspended particles (22.9 \pm 8.4%) (Fig. 3, D). For waters from both sites of Everglades, the presence of suspended particles at original concentrations did not enhance or inhibit reduction of Hg(II) under irradiation. This is likely due to the low particles' concentrations (Table S1, <3 mg/ L), and aligned with the fact that particulate Hg(0) only accounted for a minor fraction in total Hg(0) produced (Fig. 3, B and D). While such results were different from most previous studies that reported inhibiting effects of particles in Hg(II) photo-reduction (Castelle et al., 2009; Garcia et al., 2005; Tseng et al., 2004), or the few studies reporting higher photo-reduction in unfiltered waters (Amyot et al., 1997; Rolfhus and Fitzgerald, 2004), similar results have been observed (Beucher et al., 2002). They found that filtration did not affect the Hg(II) photo-reduction in tropical waters under UV irradiation, and explained that the photo-reduction was occurring in homogeneous phase without particles' involvement. However, the photo-reduction in unfiltered waters must be higher than measured, because particulate Hg(0) was not included. Therefore, their explanation that Hg(II) photo-reduction occurs in homogeneous phase may not be accurate, although the role of particles can not be assessed due to lacking information of suspended

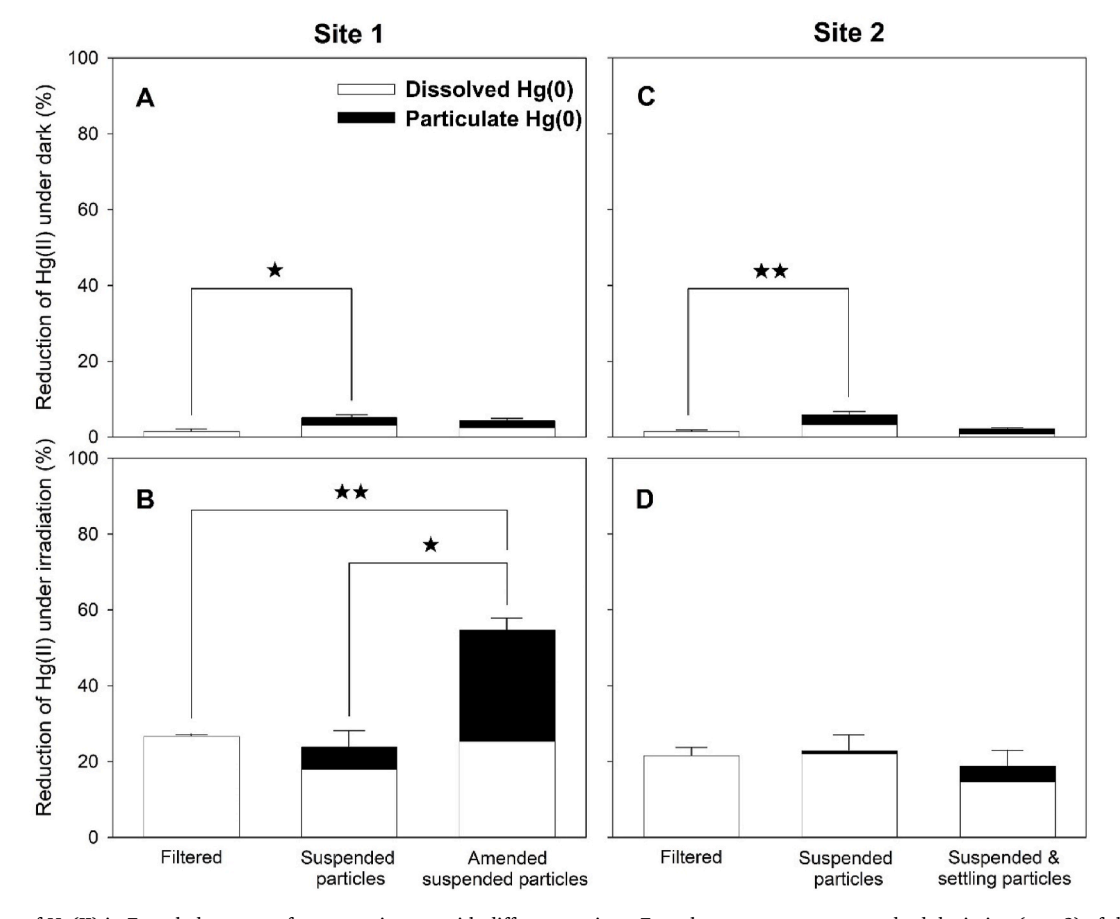


Fig. 3. Reduction of Hg(II) in Everglades waters from experiments with different settings. Error bars represent one standard deviation (n = 3) of the Hg reduction percentages. The significance lines are for *t*-test, with \star standing for p < 0.05 and $\star\star$ standing for p < 0.01.

particles and particulate Hg species. According to another study, the waters collected at the same location and season were with dissolved Hg as the predominant Hg species and suspended particles varying from 4.9 to 8.6 mg/L (Coquer et al., 2003).

For experiments using Site 1 waters, photo-reduction of Hg(II) (52.1 \pm 6.4%) in waters with amended suspended particles (14.08 mg/L) was significantly higher than in filtered waters (t-test, p < 0.01) and waters with unamended suspended particles (t-test, p = 0.01) (Fig. 3, B), suggesting the enhancing effects of suspended particles at higher concentrations on photo-reduction of Hg(II). However, such enhancing effects were not observed in experiments using Everglades waters from Site 2. In waters with amended particles, the photo-reduction of Hg(II) (18.8 \pm 8.2%) was not significantly higher than that in filtered waters or waters with suspended particles only (Fig. 3, D), despite the presence of suspended and settling particles reaching a concentration of 102.02 mg/L. Most of the particles were settling particles possessing totally different properties from suspended particles. Sush differences and their resulting differences in Hg adsorption and irradiation attenuation manifested inhibiting effects on Hg(II) photo-reduction, thus offsetting the enhancing effects of natural particles.

As shown in Panel B of Fig. 3, particulate Hg(0) accounted for a large fraction of the total Hg(0) from photo-reduction in the Site 1 waters with amended particles. Actually, the contribution from particulate Hg(0) (29.4 \pm 5.8%) was comparable (t-test, p = 0.57) to that from dissolved Hg(0) (25.3 \pm 9.8%). In Site 2 waters with suspended and settling particles, particulate Hg(0) (4.2 \pm 2.2%) accounted for a much smaller fraction in total photo-reduction of Hg(II) than dissolved Hg(0) (14.7 \pm 8.3%), despite the high concentrations of particles. If particulate Hg(0) were not considered, Hg(II) photo-reduction would be at similar levels in Site 1 waters with different conditions of particles. Therefore, the enhancing photo-reduction and large fractions of particulate Hg(0) suggested the occurrence of heterogeneous Hg(II) photo-reduction on natural particles' surfaces. However, the occurrence of particulate Hg(0) in natural waters has been largely overlooked and rarely measured (Wang et al., 2015), and previous studies on photo-reduction of Hg(II) in

natural waters have overwhelmingly focused on DGM without taking particulate Hg(0) into consideration. Given that particulate Hg(0) can compose a large fraction of total Hg(0) in natural waters, not considering particulate Hg(0) may have led to a systematic underestimate of Hg(II) photo-reduction and natural particles' enhancing effects on the reaction.

3.2. Effects of irradiation characteristics

As the energy source, irradiation directly determines photoreduction of Hg(II), either occurring homogeneously in dissolved phase or heterogeneously on particles' surfaces (Luo et al., 2020). Natural particles are known to indirectly inhibit Hg(II) photo-reduction through altering irradiation quality and intensity (Castelle et al., 2009; Vost et al., 2012). To better interpret the results of Hg(II) photo-reduction, here we analyzed the characteristics of irradiation monitored during the experiments, including the irradiation intensities (Fig. 4) and fractions of UV, Vis and NIR to total irradiation (Fig. S4). All irradiation characteristics were monitored at the bottoms of reaction bubblers, to examine the alteration of irradiation after passing through the bubblers with different waters. While the particles, DOC, waters, and the bubblers all contributed to the irradiation alteration, the different irradiation characteristics between experiments can be attributed to the particles with different conditions because all other factors were the same.

Besides those for experimental waters from the Everglades, we also measured irradiation intensity at the bottom of bubblers with MQ water as a control. Without attenuation by matrix like DOC and particles, the irradiation intensity was higher for MQ water than any Everglades waters (t-test, p < 0.05) (Fig. 4). For experiments using Everglades waters from Site 1, the irradiation intensities exhibited a high to low order of filtered waters > waters with suspended particles > waters with amended suspended particles (Fig. 4). Similar trend was observed for experiments using Site 2 waters: filtered waters > waters with suspended particles > waters with suspended particles > waters with suspended particles > waters with suspended & settling particles (Fig. 4).

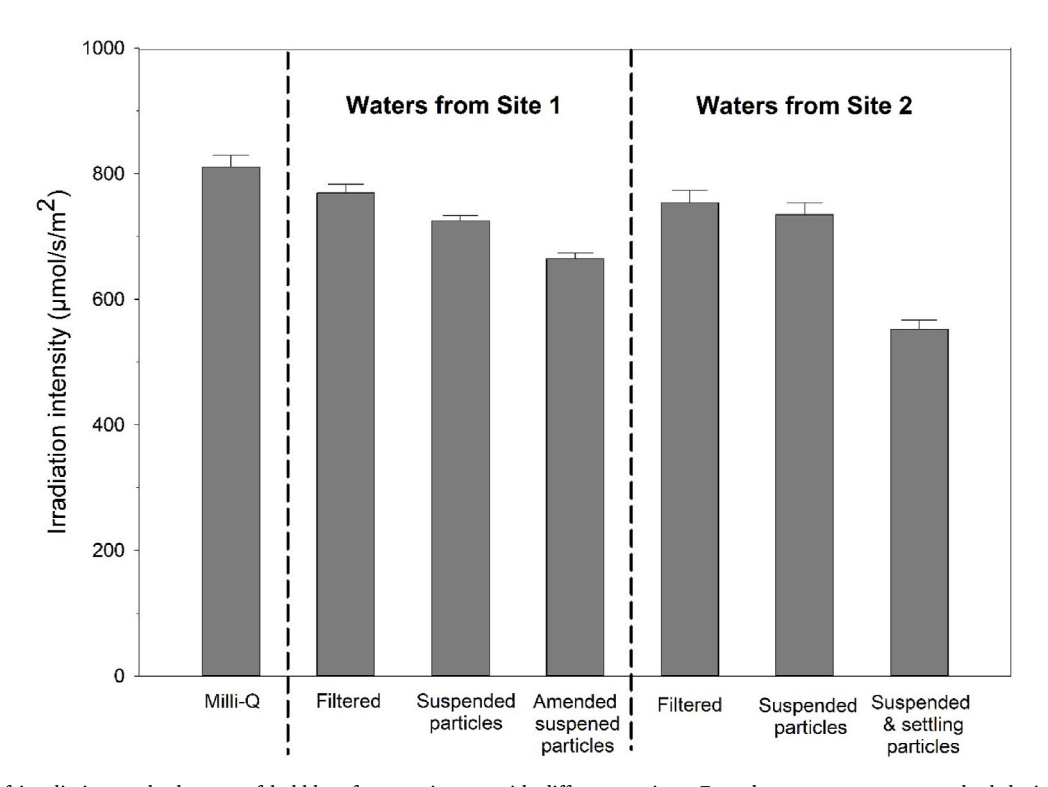


Fig. 4. Intensities of irradiation at the bottom of bubblers for experiments with different settings. Error bars represent one standard deviation (n = 3) of the irradiation intensities.

Such trends agree well with the concentration differences of particles in different waters. Comparing to those for filtered waters, irradiation intensities for waters with suspended particles exhibited slight decreases of 5.8% and 2.6% for waters from Site 1 and 2, respectively. For Site 2 waters, the intensity difference between filtered waters and waters with suspended particles was not even statistically significant (t-test, p = 0.29). The slight decreases in irradiation intensity likely resulted from low concentrations of suspended particles. When the suspended particles were amended to 6.9 times of original concentrations, the irradiation intensity dropped significantly (*t*-test, p < 0.001) to 86.4% of that in filtered Site 1 waters. Despite the substantial irradiation intensity attenuation, Hg(II) photo-reduction increased to ~2 times of those in filtered waters or waters with unamended suspended particles, demonstrating the enhancing effects of natural particles on Hg(II) photoreduction. Due to the high concentrations of suspended & settling particles (>100 mg/L), irradiation intensity was only 73.2% and 75.1% of that in filtered waters and waters with only suspended particles, respectively. The high irradiation intensity attenuation largely offset the enhancing effects of particles, and at least partially responsible for nonenhancing Hg(II) photo-reduction in waters with high concentrations of suspended & settling particles relative to those in filtered waters or waters with only suspended particles.

Not all wavelengths of irradiation contribute equally to photo-reduction of Hg(II) (Zheng and Hintelmann, 2009). Previous studies found that Vis, UVA and UVB were the main contributors to Hg(II) photo-reduction (Amyot et al., 1994), whereas UVC and NIR was not important in the reactions. Fig. S4 shows the fractions of UV, Vis, and NIR to total irradiations at the bottom of reaction bubblers. The fractions of UV plus Vis reached the highest in the control group of bubblers with MQ waters. For Everglades waters from either Site 1 or 2, the fractions of UV plus Vis showed a high to low order of filtered waters > waters with suspended particles > waters with amended particles (Fig. S4). This

pattern aligns with the increasing concentrations of particles, likely because the presence of particles led to more attenuation for irradiation at shorter wavelengths (Markager and Vincent, 2000). Given the more important roles of UV and Vis in Hg(II) photo-reduction, this pattern of UV plus Vis fractions implicated that photo-reduction would be further inhibited in waters with higher concentrations of natural particles. Therefore, the shifts of irradiation fractions may have contributed to the inhibiting effects of particles on Hg(II) photo-reduction, in addition to increasing attenuation of irradiation intensity.

3.3. Effects of particles' properties

In addition to altering irradiation characteristics, natural particles can affect Hg(II) photo-reduction through other mechanisms. One mechanism is that natural particles can alter Hg(II) reactivity for photo-reduction by forming particulate Hg species (O'Driscoll et al., 2018; Tseng et al., 2004). Another potential mechanism involves the semi-conducting minerals in natural particles that may enhance Hg(II) photo-reduction (Nriagu, 1994). Here we explore these mechanisms with the measured properties of natural particles from Everglades waters.

In natural waters, Hg species tend to bind to particles, especially those rich in organic matter (Fitzgerald et al., 2007). For Hg(II), the log values of partition coefficients (K_d) in freshwaters typically fall in the range of 4–6 (Noh et al., 2013). In this study, the partitioning of Hg species was examined for Everglades waters with different settings (Fig. 5). For Site 1 waters, log K_d varied from 4.8 to 5.2 in waters with different settings. While particulate Hg only account for 10.3% of total Hg in Site 1 waters with original concentrations of Hg and suspended particles, its fraction increased to 24.8% with 20 ng/L addition of Hg(II), and further increased to 50.1% when suspended particles were amended to \sim 5 times the original concentrations. In Everglades waters from Site

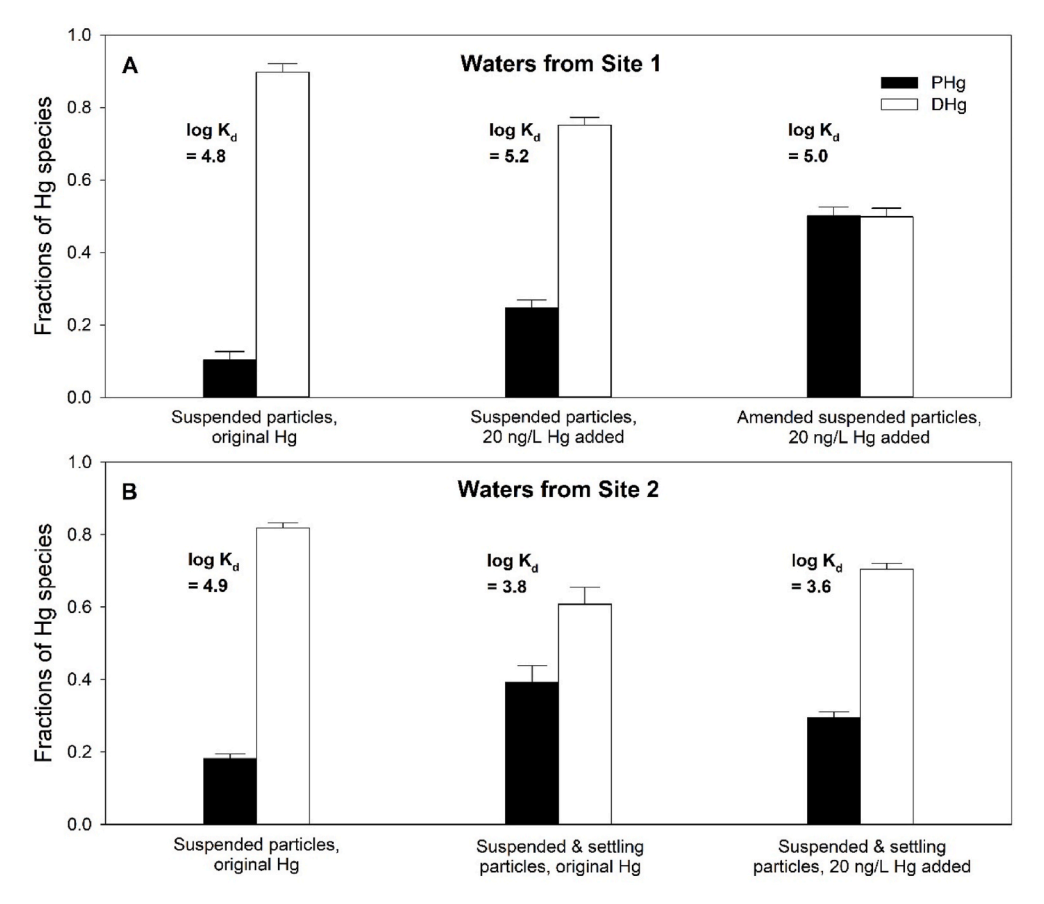


Fig. 5. Partitioning of Hg species in Everglades waters with different treatments. Error bars represent one standard deviation (n = 3) of the fractions of Hg species.

2, the log K_d for suspended particles exhibited a similar value (4.9) to Site 1 waters. The lower log K_d for suspended & settling particles (3.8, 3.6) can be partially explained by the larger sizes and thus smaller surface area-to-volume ratios of settling particles that composed most of the particles measured (Fig. S5). The size distribution patterns of particles shown in Fig. S5 were different from those in Fig. S2, likely because the particles were from waters collected at different seasons. The "particle concentration effect" (i.e., negative correlation of K_d and particle concentration) might have contributed to the lower K_d of suspended and settling particles (Cui et al., 2021; Honeyman et al., 1988). For the different K_d, another factor that might be involved was the particles' composition differences (Cui et al., 2021). The lower log K_d indicates a lower adsorption of Hg on settling particles, as supported by the fractions of Hg species in waters with different settings. Particulate Hg fraction was 18.2% in waters with original Hg and suspended particles, including settling particles did raise its fraction to 39.2%, but introducing an additional 20 ng/L Hg(II) lower this fraction to 29.5%. Therefore, in photo-reduction experiments with Hg(II) addition, particulate Hg would compose a predominant fraction of Hg species in Site 1 waters with amended suspended particles, whereas this fraction would be very limited in Site 2 waters with high concentrations of settling particles. The Hg(II) absorbed on particles was thought to be less available for photo-reduction, largely due to the premature assumption that Hg(II) photo-reduction mostly occurs in dissolved phase (Tseng et al., 2004). However, a more recent study showed that photo-reducible Hg(II) was higher with the presence of particles (O'Driscoll et al., 2018). Hence, higher fraction of particulate Hg may increase the photo-reducible Hg(II) and contribute to the enhanced photo-reduction in Site 1 waters with amended suspended particles. On the other hand, a lower particulate Hg(II) fraction may limit the photo-reduction of Hg(II) in Site 2 waters with high concentrations of suspended & settling particles. The above explanations were supported by the fractions of particulate Hg(0) in total photo-reduction of Hg(II) (Fig. 3, B and D), as detailed in Section 3.1.

The elemental composition measured with SEM-EDS showed that the major elements of the particles in mass abundance were O > Ca > C > S > Fe (Table S2), implying the minerals containing these elements as major particulate components. The mineralogy results by XRD (Fig. S6) suggested that calcite (CaCO₃) and aragonite (CaCO₃) were the major components of the suspended particles. Although ICPMS analysis indicated the presence of Fe (ranging from 0.59 to 1.6%) in the particles (agreeing with EDS results), Fe containing minerals were not detected by XRD, probably because individual Fe minerals could not reach the required level (>1% in weight) for XRD detection (Secchi et al., 2018). Taken together, the composition analysis with ICPMS, SEM-EDS, and XRD indicated the presence of Fe containing minerals, possibly Fe oxides and/or Fe sulfides. Given that SEM-EDS and XRD may not be capable of measuring low phase elements and minerals (Newbury and Ritchie, 2015; Secchi et al., 2018), respectively, we used the concentrations of metals (Table 1) by ICPMS as alternative parameters for their corresponding minerals like metal oxides and/or sulfides, which are the main semiconducting particles in natural waters (Litter et al., 1991). Here we focus on the metals contained in the minerals with E_{bg} capable of photo-reducing Hg(II), including Fe, Al, Ti, Mn and Zn. For the metals of Fe and Al, the concentrations were not significantly different among the four sources of particles. For the metals of Mn, Zn, and Ti, the concentrations were significantly lower (t-test, p < 0.01) in suspended & settling particles of Site 2 waters than in the other three sources of suspended particles. While it remains unclear whether and which semiconducting minerals enhanced Hg(II) photo-reduction, it was possible that the lower concentrations of these metals and corresponding semiconducting metal oxides limited such enhancement of photo-reduction in Site 2 waters with high concentrations of suspended & settling particles. On the other hand, the higher concentrations of these metals and corresponding semiconductors implied a stronger enhancing effect of suspended particles on Hg(II) photo-reduction. When suspended

Table 1 Metal contents of natural particles from Everglades waters. The numbers after "+/-" represent one standard deviation (n = 3) of the metal concentrations.

	Water from Site 1		Waters from Site 2	
	Suspended particles (\times 10^3 mg/kg)	Amended suspended particles (\times 10 3 mg/kg)	Suspended particles (× 10^3 mg/kg)	Suspended & settling particles ($\times 10^3$ mg/kg)
Ca	44.7 ± 35.7	35.5 ± 20.7	21.6 ± 2.42	196 ± 46.4
Al	6.09 ± 1.61	4.00 ± 1.72	64.3 ± 2.17	2.58 ± 0.221
Fe	15.9 ± 4.24	8.79 ± 0.475	6.45 ± 1.93	5.87 ± 1.17
Mn	2.18 ± 0.401	1.60 ± 0.388	0.919 ± 0.028	0.165 ± 0.039
Zn	0.368 ± 0.183	0.257 ± 0.092	0.653 ± 0.127	0.0220 ± 0.001
Ti	0.618 ± 0.240	0.717 ± 0.136	0.565 ± 0.223	0.124 ± 0.010
Cr	0.095 ± 0.036	0.099 ± 0.043	0.494 ± 0.254	0.021 ± 0.003
Cu	$\textbf{0.168} \pm \textbf{0.134}$	0.152 ± 0.073	0.195 ± 0.07	0.012 ± 0.004
Sr	0.525 ± 0.345	0.347 ± 0.195	0.303 ± 0.093	1.41 ± 0.241
Ba	0.059 ± 0.009	0.033 ± 0.010	0.087 ± 0.030	0.104 ± 0.014
K	1.75 ± 0.903	1.41 ± 0.333	2.56 ± 0.072	0.370 ± 0.239
Mg	3.96 ± 1.81	3.22 ± 1.67	3.21 ± 0.907	7.16 ± 2.76
Na	6.26 ± 1.74	3.02 ± 1.56	6.35 ± 0.039	$\textbf{0.442} \pm \textbf{0.202}$

particles were amended to 6.9 times the ambient concentration, the abundant Hg(II) absorbed on suspended particles may undergo heterogenous photo-reduction by photo-electrons from semiconductors under irradiation, thus well explaining the high particulate Hg(0) and significantly higher photo-reduction of Hg(II) (Fig. 3, B), despite multiple inhibiting effects of natural particles. It is worth noting that we conducted experiments under continuous N_2 -purging condition, in which case the generation of reactive oxygen species (ROS) and free radicals was limited (Tai et al., 2014). Therefore, the observed doubled Hg(II) reduction in suspended particle-amended Everglades water was likely due to the involvement of photo-hole and photo-electron separation and the reducing power of photo-electrons (Nriagu, 1994), rather than via ROS/free radicals-mediated pathways.

4. Conclusions

In this study, we studied the effects of natural particles on photoreduction of Hg(II) in Everglades waters using incubation experiments with additions of isotopically labelled Hg(II). Particles' effects on Hg(II) photo-reduction were not observed between filtered or unfiltered Everglades waters, probably because of the low concentrations of SPM (<3 mg/L). When suspended particles were amended to 6.9 times the ambient concentration, photo-reduction of Hg(II) was significantly enhanced to ~2 times of those in filtered waters or waters with unamended suspended particles. The abundant Hg(II) adorbed on suspended particles might be photo-reduced on particles' surfaces by photo-electrons from semiconductors under irradiation, and led to high fractions of particulate Hg(0) and significantly higher Hg(II) photoreduction in Everglades waters with amended suspended particles containing higher semiconducting minerals. However, in Site 2 Everglades waters, high concentrations (~100 mg/L) of settling particles failed to enhance Hg(II) photo-reduction. The potential enhancing effects were likely offset by inhibiting effects due to higher irradiation attenuation and lower Hg(II) partition coefficients of the settling particles with larger sizes. In addition, the lower concentrations of metals (i.e., Ti, Mn, Zn) and semiconducting minerals containing these metals may have limited the enhancing Hg(II) photo-reduction in Site 2 Everglades waters with suspended and settling particles.

The enhancing effects observed in this study demonstrated that natural particles' role was not limited to inhibiting Hg(II) photoreduction by altering irradiation intensity and quality. Meanwhile, the Hg(II) absorbed on particles are not necessarily more refractory for photo-reduction. Instead, this Hg species may induce heterogeneous photo-reduction and enhance overall Hg(II) photo-reduction in natural waters. The large fractions of particulate Hg(0) in photo-reduction

suggested that previous studies have underestimated Hg(II) photoreduction in natural waters and partly contributed to the overlooking of natural particles' enhancing effects on the reaction. While it remains unclear through what mechanism(s) increasing suspended particles enhanced Hg(II) photo-reduction in Everglades waters, the continuous N_2 -purging experimental condition limiting the generation of ROS and free radicals and the higher concentrations of metals (i.e., T_i , M_i , Z_i) seemed supporting the reduction of Hg(II) by photo-electrons from semiconducting particles under irradiation. This study highlights the direct involvements of particles in photoreaction of Hg species in natural waters and calls for more mechanistic research on heterogenous photoreduction of Hg species on particles' surfaces.

Author statement

Kang Wang: Investigation, Data curation, Writing- Original draft preparation; Guangliang Liu: Conceptualization, Data curation, Writing-Reviewing and Editing; Yong Cai: Conceptualization, Writing- Reviewing and Editing; Supervision.

Declaration of competing interest

The authors declare that they have no known competing financial interests or personal relationships that could have appeared to influence the work reported in this paper.

Data availability

Data will be made available on request.

Acknowledgements

This is contribution number 1535 from the Institute of Environment at Florida International University. Authors gratefully acknowledge National Science Foundation programs (ECS1905239) for the support of the work.

Appendix A. Supplementary data

Supplementary data related to this article can be found at https://doi.org/10.1016/j.envpol.2023.121327.

References

- Amyot, M., Gill, G.A., Morel, F.M., 1997. Production and loss of dissolved gaseous mercury in coastal seawater. Environ. Sci. Technol. 31, 3606–3611.
- Amyot, M., McQueen, D.J., Mierle, G., Lean, D.R., 1994. Sunlight-induced formation of dissolved gaseous mercury in lake waters. Environ. Sci. Technol. 28, 2366–2371.
- Ariya, P.A., Amyot, M., Dastoor, A., Deeds, D., Feinberg, A., Kos, G., et al., 2015. Mercury physicochemical and biogeochemical transformation in the atmosphere and at atmospheric interfaces: a review and future directions. Chem. Rev. 115, 3760–3802.
- Beucher, C., Wong-Wah-Chung, P., Richard, C., Mailhot, G., Bolte, M., Cossa, D., 2002. Dissolved gaseous mercury formation under UV irradiation of unamended tropical waters from French Guyana. Sci. Total Environ. 290, 131–138.
- Braude, E., 1955. Ultraviolet and visible light absorption. Determ. Org. Struct. Phys. Methods 1, 131.
- Castelle, S., Schäfer, J., Blanc, G., Dabrin, A., Lanceleur, L., Masson, M., 2009. Gaseous mercury at the air–water interface of a highly turbid estuary (Gironde Estuary, France). Mar. Chem. 117, 42–51.
- Chen, S., Wang, L.-W., 2012. Thermodynamic oxidation and reduction potentials of photocatalytic semiconductors in aqueous solution. Chem. Mater. 24, 3659–3666.
- Coquer, M., Cossa, D., Azemard, S., Peretyazhko, T., Charlet, L., 2003. Methylmercury formation in the anoxic waters of the Petit-Saut reservoir (French Guiana) and its spreading in the adjacent Sinnamary river. In: Journal de Physique IV (Proceedings) vol. 107. EDP sciences, pp. 327–331.
- Costa, M., Liss, P., 2000. Photoreduction and evolution of mercury from seawater. Sci. Total Environ. 261, 125–135.
- Cotton, F.A., Wilkinson, G., 1962. Advanced Inorganic Chemistry. John Wiley and Sons, Inc., New York, p. 876.
- Cui, X., Lamborg, C.H., Hammerschmidt, C.R., Xiang, Y., Lam, P.J., 2021. The effect of particle composition and concentration on the partitioning coefficient for mercury in three ocean basins. Front. Environ. Chem. 2, 660267.

- Dombrovsky, L.A., Solovjov, V.P., Webb, B.W., 2011. Attenuation of solar radiation by a water mist from the ultraviolet to the infrared range. J. Quant. Spectrosc. Radiat. Transf. 112, 1182–1190.
- Fitzgerald, W.F., 1999. Clean hands, dirty hands: clair Patterson and the aquatic biogeochemistry of mercury. Clean Hands: Clair Patterson's Crusade Environ. Lead Contam. 119–137.
- Fitzgerald, W.F., Lamborg, C.H., Hammerschmidt, C.R., 2007. Marine biogeochemical cycling of mercury. Chem. Rev. 107, 641–662.
- Garcia, E., Amyot, M., Ariya, P.A., 2005. Relationship between DOC photochemistry and mercury redox transformations in temperate lakes and wetlands. Geochem. Cosmochim. Acta 69, 1917–1924.
- Hammerschmidt, C.R., Bowman, K.L., Tabatchnick, M.D., Lamborg, C.H., 2011. Storage bottle material and cleaning for determination of total mercury in seawater. Limnol Oceanogr. Methods 9, 426–431.
- Hegyi, J., Horvath, O., 2004. Photocatalytic reduction of mercury (II) and simultaneous oxidative degradation of surfactants in titanium dioxide suspensions. From Colloids Nanotechnol. 10–16. Springer.
- Hines, N.A., Brezonik, P.L., 2004. Mercury dynamics in a small Northern Minnesota lake: water to air exchange and photoreactions of mercury. Mar. Chem. 90, 137–149.
- Hintelmann, H., Evans, R., 1997. Application of stable isotopes in environmental tracer studies–Measurement of monomethylmercury (CH3Hg+) by isotope dilution ICP-MS and detection of species transformation. Fresenius' J. Anal. Chem. 358, 378–385.
- Hintelmann, H., Ogrinc, N., 2003. Determination of Stable Mercury Isotopes by ICP/MS and Their Application in Environmental Studies, vol. 835. Washington D.C American Chemical Society.
- Honeyman, B.D., Balistrieri, L.S., Murray, J.W., 1988. Oceanic trace metal scavenging: the importance of particle concentration. Deep-Sea Res., Part A 35, 227–246.
- Jiang, P., Liu, G., Cui, W., Cai, Y., 2018. Geochemical modeling of mercury speciation in surface water and implications on mercury cycling in the everglades wetland. Sci. Total Environ. 640, 454–465.
- Kadi, M.W., Mohamed, R.M., Ismail, A.A., Bahnemann, D.W., 2020. Performance of mesoporous α-Fe2O3/g-C3N4 heterojunction for photoreduction of Hg (II) under visible light illumination. Ceram. Int. 46, 23098–23106.
- Korsman, T., Renberg, I., Dåbakk, E., Nilsson, M.B., 2002. Near-infrared spectrometry (NIRS) in palaeolimnology. Track. Environ. Change Lake Sediment. 299–317. Springer.
- Kritee, K., Blum, J.D., Barkay, T., 2008. Mercury stable isotope fractionation during reduction of Hg (II) by different microbial pathways. Environ. Sci. Technol. 42, 9171–9177.
- Lamborg, C.H., Hansel, C.M., Bowman, K.L., Voelker, B.M., Marsico, R.M., Oldham, V.E., et al., 2021. Dark reduction drives evasion of mercury from the ocean. Front. Environ. Chem. 2, 659085.
- Lamborg, C.H., Tseng, C.-M., Fitzgerald, W.F., Balcom, P.H., Hammerschmidt, C.R., 2003. Determination of the mercury complexation characteristics of dissolved organic matter in natural waters with "reducible Hg" titrations. Environ. Sci. Technol. 37, 3316–3322.
- Le Roux, S.M., Turner, A., Millward, G.E., Ebdon, L., Appriou, P., 2001. Partitioning of mercury onto suspended sediments in estuaries presented at the Whistler 2000 speciation Symposium, Whistler Resort, BC, Canada, June 25–July 1, 2000.
 J. Environ Monit 3, 37–42
- Li, L., Wang, X., Fu, H., Qu, X., Chen, J., Tao, S., et al., 2020. Dissolved black carbon facilitates photoreduction of Hg (II) to Hg (0) and reduces mercury uptake by lettuce (Lactuca sativa L.). Environ. Sci. Technol. 54, 11137–11145.
- Litter, M.I., Baumgartner, E.C., Urrutia, G.A., Blesa, M.A., 1991. Photodissolution of iron oxides. 3. Interplay of photochemical and thermal processes in maghemite/carboxylic acid systems. Environ. Sci. Technol. 25, 1907–1913.
- Liu, G., Cabrera, J., Allen, M., Cai, Y., 2006. Mercury characterization in a soil sample collected nearby the DOE Oak Ridge Reservation utilizing sequential extraction and thermal desorption method. Sci. Total Environ. 369, 384–392.
- Liu, G., Cai, Y., Philippi, T., Kalla, P., Scheidt, D., Richards, J., et al., 2008. Distribution of total and methylmercury in different ecosystem compartments in the Everglades: implications for mercury bioaccumulation. Environ. Pollut. 153, 257–265.
- Luo, H., Cheng, Q., Pan, X., 2020. Photochemical behaviors of mercury (Hg) species in aquatic systems: a systematic review on reaction process, mechanism, and influencing factor. Sci. Total Environ., 137540
- Markager, S., Vincent, W.F., 2000. Spectral light attenuation and the absorption of UV and blue light in natural waters. Limnol. Oceanogr. 45, 642–650.
- Meija, J., Yang, L., Sturgeon, R.E., Mester, Z., 2010. Certification of natural isotopic abundance inorganic mercury reference material NIMS-1 for absolute isotopic composition and atomic weight. J. Anal. At. Spectrom. 25, 384–389.
- Mohamed, R.M., Ismail, A.A., 2021. Mesoporous α -Fe2O3/ZnO heterojunction with a synergistic effect for rapid and efficient reduction of mercury ions. Separ. Purif. Technol. 266, 118360.
- Moradi, H., Abtahi, A., Zilouchian, A., 2017. Financial analysis of a grid-connected photovoltaic system in South Florida. In: 2017 IEEE 44th Photovoltaic Specialist Conference (PVSC). IEEE, pp. 638–642.
- Munson, K.M., Lamborg, C.H., Swarr, G.J., Saito, M.A., 2015. Mercury species concentrations and fluxes in the central tropical Pacific ocean. Global Biogeochem. Cycles 29, 656–676.
- Newbury, D.E., Ritchie, N.W., 2015. Performing elemental microanalysis with high accuracy and high precision by scanning electron microscopy/silicon drift detector energy-dispersive X-ray spectrometry (SEM/SDD-EDS). J. Mater. Sci. 50, 493–518.
- Noh, S., Choi, M., Kim, E., Dan, N.P., Thanh, B.X., Van Ha, N.T., et al., 2013. Influence of salinity intrusion on the speciation and partitioning of mercury in the Mekong River Delta. Geochem. Cosmochim. Acta 106, 379–390.

- Nriagu, J.O., 1994. Mechanistic steps in the photoreduction of mercury in natural waters. Sci. Total Environ. 154, 1–8.
- O'Driscoll, N., Siciliano, S., Lean, D., Amyot, M., 2006. Gross photoreduction kinetics of mercury in temperate freshwater lakes and rivers: application to a general model of DGM dynamics. Environ. Sci. Technol. 40, 837–843.
- O'Driscoll, N.J., Vost, E., Mann, E., Klapstein, S., Tordon, R., Lukeman, M., 2018. Mercury photoreduction and photooxidation in lakes: effects of filtration and dissolved organic carbon concentration. J. Environ. Sci. 68, 151–159.
- Pataki, L., Zapp, E., 2013. Basic Analytical Chemistry. Elsevier Science, p. 140.
 Pućko, M., Burt, A., Walkusz, W., Wang, F., Macdonald, R., Rysgaard, S., et al., 2014.
 Transformation of mercury at the bottom of the Arctic food web: an overlooked puzzle in the mercury exposure narrative. Environ. Sci. Technol. 48, 7280–7288.
- Qureshi, A., MacLeod, M., Hungerbühler, K., 2011. Quantifying uncertainties in the global mass balance of mercury. Global Biogeochem. Cycles 25.
- Rolfhus, K.R., Fitzgerald, W.F., 2004. Mechanisms and temporal variability of dissolved gaseous mercury production in coastal seawater. Mar. Chem. 90, 125–136.
- Saiz-Lopez, A., Acuña, A.U., Trabelsi, T., Carmona-García, J., Dávalos, J.Z., Rivero, D., et al., 2019. Gas-phase photolysis of Hg (I) radical species: a new atmospheric mercury reduction process. J. Am. Chem. Soc. 141, 8698–8702.
- Saniewska, D., Bełdowska, M., Bełdowski, J., Saniewski, M., Szubska, M., Romanowski, A., et al., 2014. The impact of land use and season on the riverine transport of mercury into the marine coastal zone. Environ. Monit. Assess. 186, 7593–7604.
- Secchi, M., Zanatta, M., Borovin, E., Bortolotti, M., Kumar, A., Giarola, M., et al., 2018. Mineralogical investigations using XRD, XRF, and Raman spectroscopy in a combined approach. J. Raman Spectrosc. 49, 1023–1030.
- Si, L., Branfireun, B.A., Fierro, J., 2022. Chemical oxidation and reduction pathways of mercury relevant to natural waters: a review. Water 14, 1891.
- Skubal, L., Meshkov, N., 2002. Reduction and removal of mercury from water using arginine-modified TiO2. J. Photochem. Photobiol. Chem. 148, 211–214.
- Southworth, B., Hodecker, J., Fleischer, K., 1958. Determination of mercury in organic compounds. A micro and semimicromethod. Anal. Chem. 30, 1152–1153.
- Starr, D.E., Favaro, M., Abdi, F.F., Bluhm, H., Crumlin, E.J., van de Krol, R., 2017.

 Combined soft and hard X-ray ambient pressure photoelectron spectroscopy studies

- of semiconductor/electrolyte interfaces. J. Electron. Spectrosc. Relat. Phenom. 221, 106–115.
- Tai, C., Li, Y., Yin, Y., Scinto, L.J., Jiang, G., Cai, Y., 2014. Methylmercury photodegradation in surface water of the Florida Everglades: importance of dissolved organic matter-methylmercury complexation. Environ. Sci. Technol. 48, 7333–7340.
- Tseng, C., Lamborg, C., Fitzgerald, W., Engstrom, D., 2004. Cycling of dissolved elemental mercury in Arctic Alaskan lakes. Geochem. Cosmochim. Acta 68, 1173–1184.
- Tsui, M.T.-K., Blum, J.D., Kwon, S.Y., 2020. Review of stable mercury isotopes in ecology and biogeochemistry. Sci. Total Environ. 716, 135386.
- UNEP/AMAP, 2013. Technical Background Report for the Global Mercury Assessment. Vost, E.E., Amyot, M., O'Driscoll, N.J., 2012. Photoreactions of mercury in aquatic systems. Environ. Chem. Toxicol. Mercury 193–218.
- Wang, K., Liu, G., Cai, Y., 2022. Possible pathways for mercury methylation in oxic marine waters. Crit. Rev. Environ. Sci. Technol. 52, 3997–4015.
- Wang, K., Munson, K.M., Armstrong, D., Macdonald, R.W., Wang, F., 2020. Determining seawater mercury methylation and demethylation rates by the seawater incubation approach: a critique. Mar. Chem. 219, 103753.
- Wang, X., Pehkonen, S., Ray, A.K., 2004. Photocatalytic reduction of Hg (II) on two commercial TiO2 catalysts. Electrochim. Acta 49, 1435–1444.
- Wang, Y., Li, Y., Liu, G., Wang, D., Jiang, G., Cai, Y., 2015. Elemental mercury in natural waters: occurrence and determination of particulate Hg (0). Environ. Sci. Technol. 49, 9742–9749.
- Wu, B., Zhou, C., Zhao, G., Wang, J., Dai, H., Liu, T., et al., 2022. Enhanced photochemical production of reactive intermediates at the wetland soil-water interface. Water Res. 223, 118971.
- Zhang, H., 2006. Photochemical redox reactions of mercury. Rec. Dev. Mercury Sci. 37–79. Springer.
- Zhang, H., Lindberg, S.E., 2001. Sunlight and iron (III)-induced photochemical production of dissolved gaseous mercury in freshwater. Environ. Sci. Technol. 35, 038, 035
- Zheng, W., Hintelmann, H., 2009. Mercury isotope fractionation during photoreduction in natural water is controlled by its Hg/DOC ratio. Geochem. Cosmochim. Acta 73, 6704–6715